COMPDYN 2015
5th ECCOMAS Thematic Conference on
Computational Methods in Structural Dynamics and Earthquake Engineering
M. Papadrakakis, V. Papadopoulos, V. Plevris (eds.)
Crete Island, Greece, 25–27 May 2015

POUNDING BETWEEN BRIDGE DECKS: COMPUTATIONAL DETAILS AND RESULTS

Bharat Mandal[1*], Vincenzo Bianco[1], and Giorgio Monti[1]

[1] Sapienza University of Rome
Department of Structural Engineering and Geotechnics
Via Antonio Gramsci 53 – 00197 – Rome - Italy
*bharatmandal@yahoo.com

Keywords: Pounding, bridge decks, numerical modelling, response spectrum.

Abstract. *The observation of damage to structures, either buildings or bridges, due to earthquake induced pounding, dates back to early San Fernando (1971) and Mexico City (1985) post-earthquake reconnaissance reports. Recent ground shakings that have struck Italian territories have renewed the awareness of the necessity to clarify some aspects related to the pounding-induced forces acting on the bridge and viaduct piers. Historically pounding has been studied by either of two approaches, that are: 1) the stereo-mechanical approach, based on the physical laws of the impact phenomenon and the definition of a restitution factor, and 2) the force-based approach, based on the definition of the local force due to impact. Moreover, impact can be either soft or hard, depending on the amount of earthquake-induced energy dissipated locally through the damage of the colliding bodies. In this study, pounding response of two linear SDOF (Single Degree Of Freedom) systems has been studied through different models, namely: 1) Linear Spring, 2) Kelvin-Voigt, 3)Hertz, 4) Hertz-damp and 5) Stereo-mechanical model. Those models have been applied using both backward and forward spectrum-compatible and artificially generated ground motions. After introducing 1) the details of each of those models, 2) the main differences among them, and 3) the numerical computational strategy implemented, the main results are presented. Among these latter, being the early results of an exploratory and propaedeutic work for a Doctoral Thesis, the pounding-inducted response spectra, either in terms of peak displacement or pounding force, are developed.*

1 INTRODUCTION

Pounding is the cyclic hammering that can occur, during a seismic event, between close structures oscillating out-of-phase when the gap between these latter is not large enough to accommodate their earthquake-induced horizontal displacements.

It is a phenomenon that has been largely documented in the past, as a major cause of both buildings and bridges collapses during earthquakes (*e.g.* [1-8]). In particular, as to the bridges, impact between decks and abutments had already been observed in the 1971 San Fernando earthquake [1]. In the 1994 Northridge earthquake, at a location approximately 12 km far from the epicenter, significant pounding damage was observed at the expansion hinges and abutments of the still standing portions of a number of bridges [4]. During the 1995 Hyogo-Ken Nanbu earthquake in Kobe, Japan, several pounding-related failures had occurred: 1) longitudinal movements of the elements of the Hanshin Expressway superstructure reached almost 30 cm and caused considerable pounding damage at the expansion joints, 2) span collapse due to restrainer failure, and 3) fracture of the bearing supports causing the collapse of several decks [5]. Reconnaissance visits after the 1999 Sep 21 Chi-Chi earthquake in Taiwan revealed hammering at the expansion joints in some bridges which resulted in damage to shear keys, bearings and anchor bolts [6]. During the 2001 Bhuj earthquake, in India, a large number of railway and highway bridges were damaged. A number of reinforced concrete slab culverts on stone masonry abutments sustained damage at the seating of the span. Adjacent spans having girder/slab with different depths, were severely damaged. The large movement of the girders along either the longitudinal or the transversal direction imposed severe strains on the neoprene bearings [7].

From these field observations some general conclusions can be drawn about the typical pounding damages induced to bridges, which can comprehend (Fig. 1): 1) bearing damage, for either longitudinal or transversal earthquake, with consequent unseating and bridge collapse; 2) amplification of longitudinal displacements with consequent unseating; 3) damage to both the abutment and piers transversal retainers; 4) local damage to the impacting decks surfaces, typically summarized as concrete spalling, in its lightest form; 5) shear failure at the abutment beneath the fixed supports; 6) damage to the piers due to excessive displacements imposed.

The kind of damage undergone by a case-study bridge can depend on a number of parameters, both geometrical and mechanical. Moreover, based on these latter, impact between colliding parts can be classified as *soft* impact or *hard* impact. Where the former refers to the case in which most of the energy is dissipated locally, through local damage, while the latter refers to the case in which, due to the high stiffness of the colliding bodies, energy lost locally is negligible with respect to the amount of energy transferred to the impacting bodies in terms of momentum, which results in this way predominant. In this latter case, more likely for the longitudinal impact, the large horizontal force transferred from one deck to the adjacent one, can result in a significant change in the dynamic behavior of the entire bridge.

In this work attention is focused on the case of Reinforced Concrete (RC) viaducts composed of simply supported girders in series (Fig. 2). In this case the two adjacent spans, each with its restrained pier, in correspondence of the beam hinge extremity, can be modelled by two adjacent SDOF systems connected by an impact element.

Attention is first focused on the numerical modelling strategies available in the literature and, in the second part of the paper, the early results of a propaedeutic work for a Doctoral thesis are presented. Attention is dedicated to the possibility to produce spectra, either providing the maximum displacement or force, induced by pounding, during an earthquake. In fact,

spectra can be a very useful analytical tool for practicing engineers committed with the design or rehabilitation of bridges in seismic-prone areas [9].

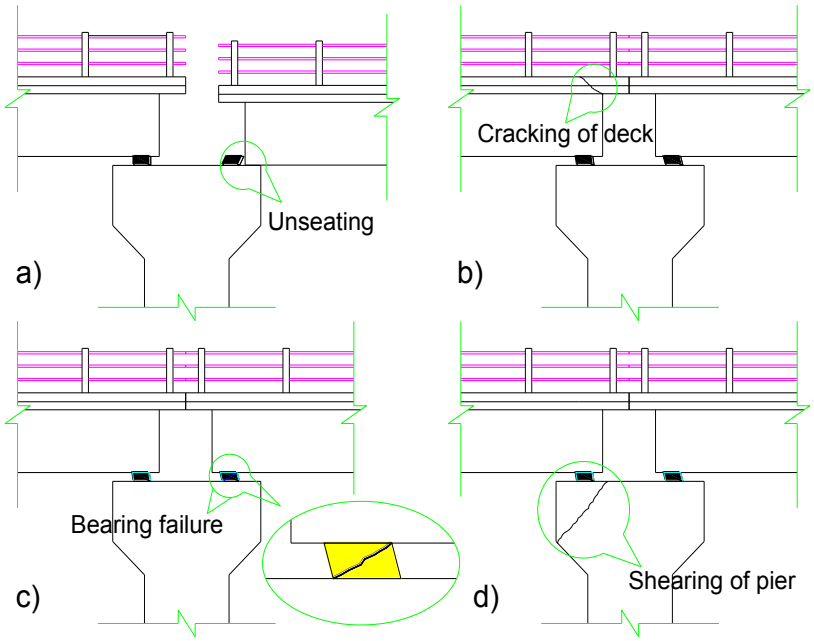

Figure 1: Examples of damage due to earthquake-induced pounding: a) unseating of girder, b) shear cracking of deck, c) bearing shear failure and d) shearing of pier/abutment.

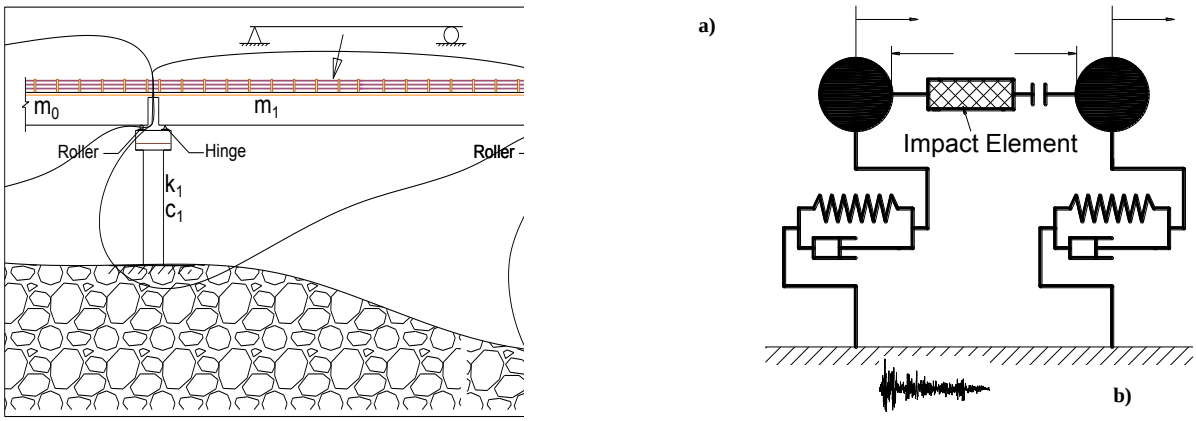

Fig. 2. Idealized Model of bridge: a) adjacent bridge segments, and b) two SDOF model with impact element.

2 POUNDING MODELS AVAILABLE IN THE LITERATURE

Pounding phenomenon has attracted the attention of academic community in the last decades and a relatively large amount of specific scientific literature has already been produced (*e.g.* [10-21]).

The equations of motion representing the dynamic equilibrium of the two colliding masses subject to earthquake can be written as follows:

(1)

where: m_1 and m_2 are the mass of first and second colliding bodies, respectively; and are the relevant damping values; k_1 and are the horizontal displacement stiffness of the vertical structures supporting the first and second mass, respectively; is the ground acceleration and is the pounding force arising locally in the instant of impact; $x_1(t)$ and (t) are the time step-dependent values the two masses displacements while the first derivatives ($\dot{x}_1$, $\dot{x}_2$) and the second derivatives ($\ddot{x}_1$, $\ddot{x}_2$) are the velocities and accelerations respectively. In a time step-wise implementation, impact occurs at each time instant t in which the following inequality is fulfilled (Fig. 2):

(2)

where: δ is the measure of the penetration, g_p is the gap among the two colliding masses.

From a numerical point of view, pounding has been traditionally studied by either one of two models, that are: a) stereo-mechanical, or b) force-based.

2.1 Stereo-Mechanical Model (SMM)

The Stereo-mechanical model is based on the use of: a) the momentum conservation principle and b) the coefficient of restitution, e. The former can be written as:

(3)

where: ($\dot{x}_1'$, $\dot{x}_2'$) and ($\dot{x}_1$, $\dot{x}_2$) are the velocity values after and before impact, respectively. This principle means that the momentum after impact is equal to the momentum before impact. The coefficient of restitution, which is the ratio of the relative velocity after impact to the relative velocity before impact, is given by:

(4)

and gives a measure of the energy loss during impact. In fact it varies between 0, meaning perfectly plastic impact occurred, and 1.0, which means that impact was perfectly elastic. In the former case, the two masses get stuck during impact and move together afterwards while, in the latter, the two masses undergo maximum rebound with no energy loss during impact. With this approach, the impact duration time is neglected and impact is considered central and without any transient stresses and deformations in the impacting bodies.

At each time step in which Eq. (2) is fulfilled, the two bodies velocities are modified according to the following expressions:

(5)

2.2 Force-based models

In the force-based models, the local impact force F_p of Eq. (1) is different than zero and evaluated as function of the penetration value $\delta(t)$. Different models simply differ by the way its dependence on the gap value is defined. Some of the alternatives adopted by so far by other researchers are reported hereinafter.

2.2.1. Linear Spring Model (LSM)

This model is the simplest since it assumes a linear dependence of on δ. The impact force is evaluated by:

for

for (6)

where the linear spring stiffness k_L is proportional to the axial stiffness of the colliding bodies. Typical values of k_L range from $8.76x10^8\ N/m$ to $5.25x10^9\ N/m$ for bridge decks [18]. This model cannot account for the energy loss during impact so that it is more indicated for analyzing the *hard impact*.

2.2.2. Linear viscous-elastic model or Kelvin-Voigt Model (KM)

The linear viscous elastic model, also known as Kelvin–Voigt model [18-19], consist in modelling the impact element by a rheological model comprehending a linear spring in parallel with a viscous damper. The linear spring has stiffness k_k and the viscous damper is characterized by the damping coefficient c_k that accounts for the local energy dissipation during impact. The impact force is given by:

for

for (7)

where $(\dot{x_1} - \dot{x_2})$ is the relative velocity. The value of can be evaluated as function of the coefficient of restitution e of Eq. (4), by the following expression:

$\xi \cdot$ (8)

where the coefficient ξ is given by:

$\xi =$ (9)

Provided that it depends on both geometry and mechanical properties of the impacting bodies, some authors [19,20] suggest the value of $k_k = 9.35x10^7\ N/m$ for $e = 0.65$ and $/m$, for $e = 0.64$. With respect to the linear model it offers the advantage of allowing the local energy loss to be accounted for even if, in some cases, it generates tensile forces acting on the bodies just before separation [18,19].

2.2.3. Non Linear model or Hertz Model (HM)

According to this model, also known as Hertz model, the impact element is composed of a non-linear spring with stiffness k_h, so that the impact force is evaluated by:

for for

for for (10)

where n is the Hertz coefficient, which is typically assumed as equal to $3/2$, since previous studies showed that the system displacement is relatively insensitive to it [21]. The impact stiffness k_h depends on both the geometrical and mechanical properties of the colliding masses. The value of k_h, suggested by some authors and based on small scale experiments [22], typically ranges from ¯ to ¯. Other authors [20] identified, through an optimization technique, a value of ¯ with $e = 0.64$.

This model allows, with respect to the Linear model, a more faithful representation of the impact force, but has the disadvantage of neglecting the local energy loss due to plastic deformation, local cracking and friction during impact.

2.2.4. Non Linear viscous-elastic model or Hertz-Damp Model (HDM)

According to this model, the impact element is composed of a non-linear spring, following the Hertz Law of contact [19] and characterized by stiffness k_{hd}, in parallel with a viscous non-linear damper, with viscous coefficient c_{hd}. The viscous damper is activated only during the approaching phase of the collision, when the colliding bodies are actually approaching each other ($(\dot{x_1} - \dot{x_2}) > 0$), in order to simulate the energy loss typically occurring during this phase [19]. On the contrary, it is deactivated during the contact restitution phase, when the colliding bodies are moving away from each other ($(\dot{x_1} - \dot{x_2}) \leq 0$). The impact force can be evaluated by the following expression:

for

for (11)

for

where the Hertz coefficient is assumed equal to $n = 3/2$; the stiffness coefficient k_{hd} depends on both mechanical and geometrical properties of the colliding bodies. The damping coefficient $c_{hd}(t)$ can be evaluated by:

(12)

where the damping ratio ξ can be evaluated, as function of e that accounts for the energy dissipation during collision, by the following approximate expression:

$$\xi = \frac{\bar{}}{} \quad (13)$$

Some author [19] suggests the value of impact stiffness $k_{hd} = 2.75 \times 10^9\ N/m^{\bar{2}}$, obtained by experimental data fitting of the maximum recorded impact force and for a value of .65. Other authors [22] suggest, for RC impacting structures, a value ranging from ¯ to ¯.

Even though more computationally demanding than the models presented in previous sections, this is expected to be the more accurate modelling strategy, as confirmed by works based on experimental and numerical comparisons [19].

3 ADOPTED BRIDGE MODEL

For the studies herein presented, a viaduct made by a series of simply supported prestressed RC girders with $50\ m$ span length and simply supported was taken into consideration (Fig. 2a). Attention was focused on the longitudinal pounding between two adjacent decks, each hinged to the relevant pier cap. Pounding between these latter was studied by the simple model (Fig. 2a) composed of two SDOF systems placed at a distance equal to the longitudinal gap between decks across the pier cap. The mass of each SDOF comprehending the deck only, was assumed equal to $2.04 \times 10^6\ kg$. The horizontal flexibility of the hinged pier was modelled, for each SDOF, by a horizontal elastic spring characterized by stiffness k_{SDOF}. The damping capability of each SDOF was modelled by a dashpot, characterized by a damping ratio, $\zeta = 5\%$. A parametric study was carried out in order to figure out the typical range of variation of the lateral stiffness of RC piers [23]. From these latter results it arose that the natural vibration period of piers typically ranges from $T = 0.2\ sec$ to $T = 4.0\ sec$.

In this section the results of some preliminary analyses, which were carried out in order to compare the results obtainable by the various pounding models presented above, are presented (Fig. 3). Vibration periods of the two SDOFs were assumed equal to $T_1 = 2\ sec$ and T sec, for the first and second mass, respectively. The recorded *El Centro* earthquake accelerogram was assumed to simulate the ground shaking (Fig. 3a). The gap was assumed equal to $g_p = 5\ cm$.

3.1 Numerical implementation

Due to the presence of earthquake-induced instantaneous pulse values of force, pounding phenomenon is governed by highly non-linear equations, so that it can only be solved by numerical methods. Herein, a stepwise numerical solving algorithm, which combines a fourth order Runge-Kutta Method (*RK4*) with a Predictor-Corrector Method, was employed. Where the *RK4* (*e.g.* [24-25]) is a a) one-step and b) explicit, numerical method. In fact, a) at current time step , *RK4* uses derivative information concerning only the beginning of the step, and b) the solving expression is explicit since it only depends on the value assumed by the variable at the beginning of the time step $x(t_i)$ so as not to necessitate iteration.

First of all, by means of the so-called State Space Formulation, Eq. (1) can be transformed into a system of four first order Ordinary Differential Equations (*ODEs*). In fact, for the *j*-th mass ($j = 1,2$), by the following positions:

(14)

the relevant 2nd order ordinary equation of Eq. (1), can be transformed in the following system of two 1st order ODEs:

(15)

At the generic time step t_{i+1}, the incremental value of displacement and velocity are obtained by the *RK4* expression, herein reported for the displacement only, for the sake of brevity:

(16)

where h is the incremental time step (single valued), and k^1 to k^4 are the *RK4* incremental coefficients, evaluated a) once on the initial instant of the time step (k^1), b) twice on the middle instant of the time step (k^2, and k^3), and c) once on the final instant of the time step (k^4), as indicated by the following expressions:

(17)

Within the generic incremental time step, after having evaluated the current value of displacements $x_1(t_{i+1})$ and $x_2(t_{i+1})$ initially assuming $F_p = 0$ in Eq. (15) (*predictor phase*), the check for pounding occurrence is carried out by Eq. (2) and, if pounding actually occurs, the actual values of displacements are re-calculated by the above numerical strategy substituting the current value of $F_p \neq 0$ into Eq. (15) (*corrector phase*). When the Stereo-mechanical method was implemented, the corrector phase was implemented by updating the current value of the velocities by Eq. (5).

3.2 Differences among pounding models

A parametric study was carried out in order to assess the variation of the peak displacement of each mass as function of a) the adopted pounding model, and b) the relevant value of the stiffness coefficient (Fig. 3). In particular: Figs. 3b and 3e represent the peak displacements, for the 1st and 2nd SDOF respectively, for each of the four force-based models and for increasing values of the impact stiffness, while Figs. 3c and 3f plot the variation of the peak displacement, for the 1st and 2nd SDOF respectively, obtained for varying values of the restitution coefficient. The results obtained by the force-based models assuming singular values of impact stiffness, suggested by other authors [19,20] are also plotted (markers in Figs. 3b, e). From the obtained results it arises that, for each force-based model, the peak displacement response is almost independent of the value assumed for the relevant impact stiffness. Overall, independently of the force-based model, the peak displacement of the 1st SDOF (stiffer) is smaller than that of the 2nd SDOF. Variation of the peak response obtained by varying the value of the restitution coefficient, in the ambit of the Stereo-mechanical model, is larger with respect to the force-based models. Anyway, it has to be pointed out that the same response as that obtained by either of the force-based models can be obtained by the Stereo-mechanical model assuming a suitably calibrated value of e. Note also that 1) the largest peak displace-

ment response is obtained by the linear model, for either SDOF, with respect to the more complicated models, and 2) the smallest peak displacement is obtained by the Hertz-damp model. This is due to the fact that the linear force-based model completely neglects local energy losses, resulting in this way more indicated for hard impact. The opposite happens for the Hertz-damp model that ends up providing the smallest peak displacement, since it allows the local energy loss to be accounted for by the impact damping coefficient. Provided that the correct value of the pounding damping is assumed, the Hertz-damp model allows also to model the case of soft impact yielding, in this way, the most correct results.

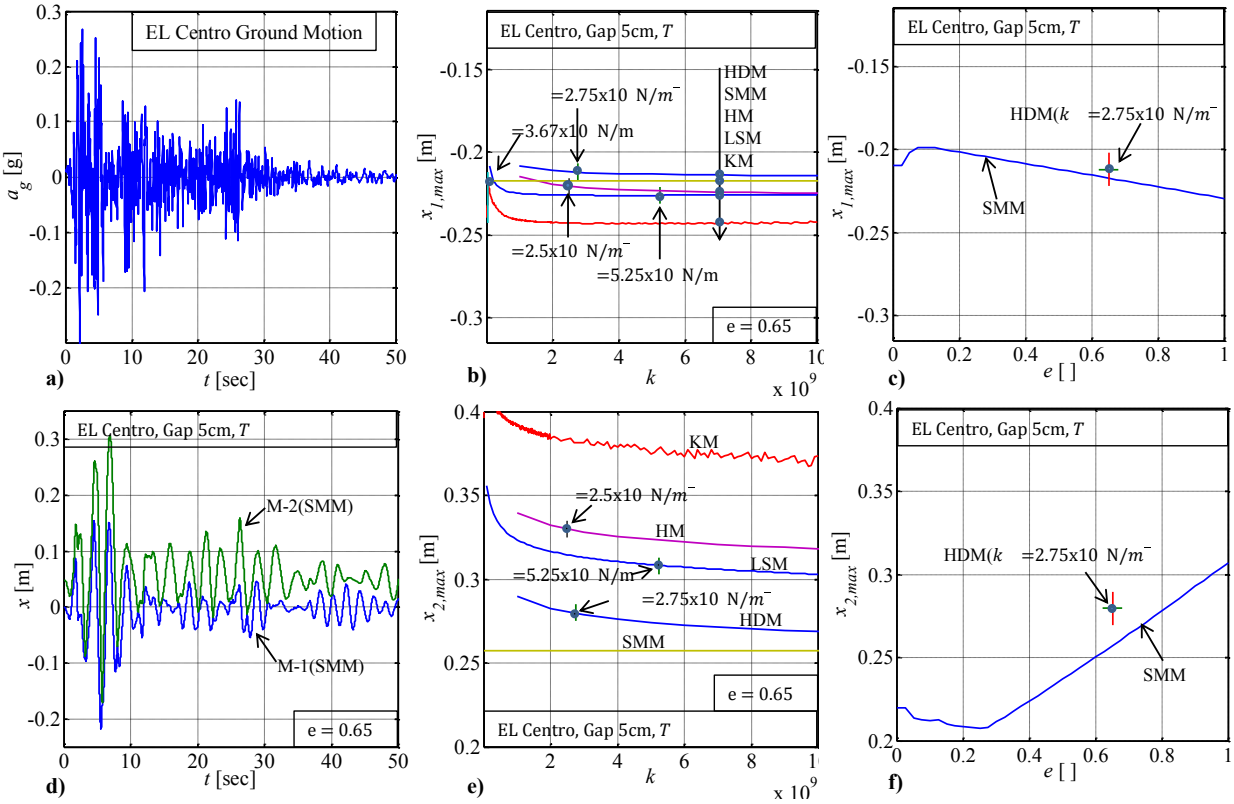

Figure 3: Comparison of Pounding Models: a) *El Centro* recorded ground motion; d) displacement response time-history for the two SDOFs for SMM with $e = 0.65$; maximum displacement response of the 1st SDOF and the 2nd SDOF obtained for (b,e) the various force-based models and for (c,f) the various values of the restitution coefficient by means of the Stereo-mechanical model.

4 RESULTS

In this section the results obtained applying the Hertz-damp model with impact stiffness value , and damping coefficient evaluated on the basis of 65 [19] are presented. Twenty spectrum compatible accelerograms were generated by SIMQKE software [26]. These latter were generated for the three soil type (A, B and D) and for three seismic zones (1, 2 and 3) contemplated by one of the more recent Italian Codes [27]. The so obtained ground motions were characterized by 25 sec overall duration, with 3 rising part and 20 sec of stationary duration. Since it was observed that earthquake direction can affect the maximum response [23], both forward and backward seismic attacks were considered. The results of the numerous analyses carried out were plotted in the form of spectra, both in terms of peak displacement (Figs. 4,5) and in terms of peak pounding force (Figs. 6,7).

In Fig. 4 the peak displacement spectrum of the 1st SDOF is plotted for different values of T_2, for Zone 1 and Soil A, and compared with the equivalent spectrum in the absence of pounding. As can be gathered, in general terms, pounding can yield either an amplification or a de-amplification with respect to the case of absence of pounding. Moreover, it can be noticed that peak displacement undergoes amplification for values of $T_1 > T_2$ which means that pounding induced amplification of the seismic response, in terms of displacements, mainly concerns the more flexible out of the two colliding bodies. This means that the tallest pier will be subjected to the largest pounding induced displacement amplification. On the contrary, the stiffer, among the two colliding SDOFs, always undergoes displacement reduction with respect to the case of absence of pounding.

The peak displacement spectrum $x_{1,max}(T_1)$ is plotted in Fig. 5 for different seismic zones (rows) and soil types (columns) and for increasing values of T_2. As can be gathered, given a seismic zone, the displacement amplification increases for decreasing mechanical characteristics of the foundation soil. In fact, for zone 1, changing the soil type from a bedrock (A) to a softer soil (D), the average spectrum of the band composed of the spectra for decreasing values of T_2, almost quadruples.

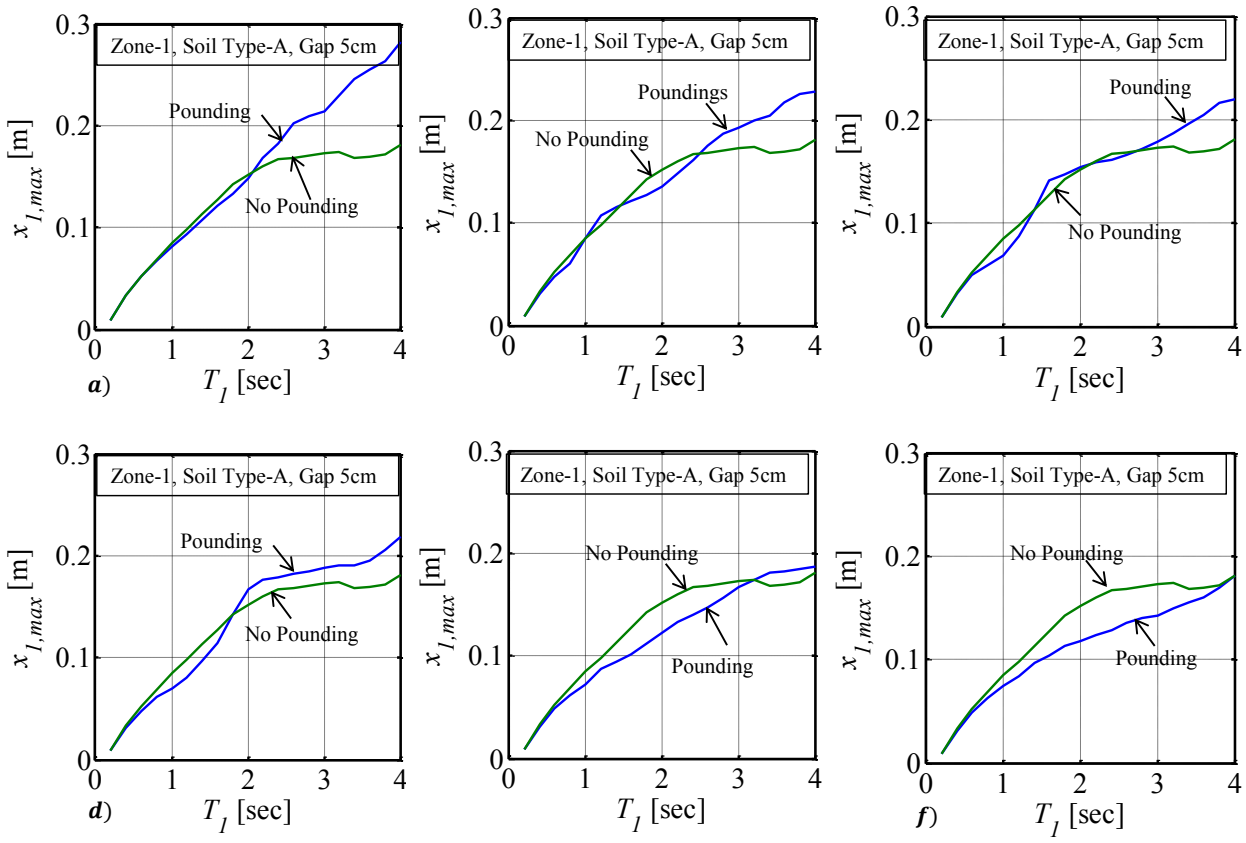

Figure 4: Non-pounding (red line) and pounding (blue line) displacement response spectra for Zone-1 and Soil Type-A for Gap size = 5cm and for different values of T_2: a)$T_2 = 0.2sec$; b) $T_2 = 1.0sec$; c) $T_2 = 1.4sec$; d) ec; e)$T_2 = 3.2sec$; f) $T_2 = 4.0sec$.

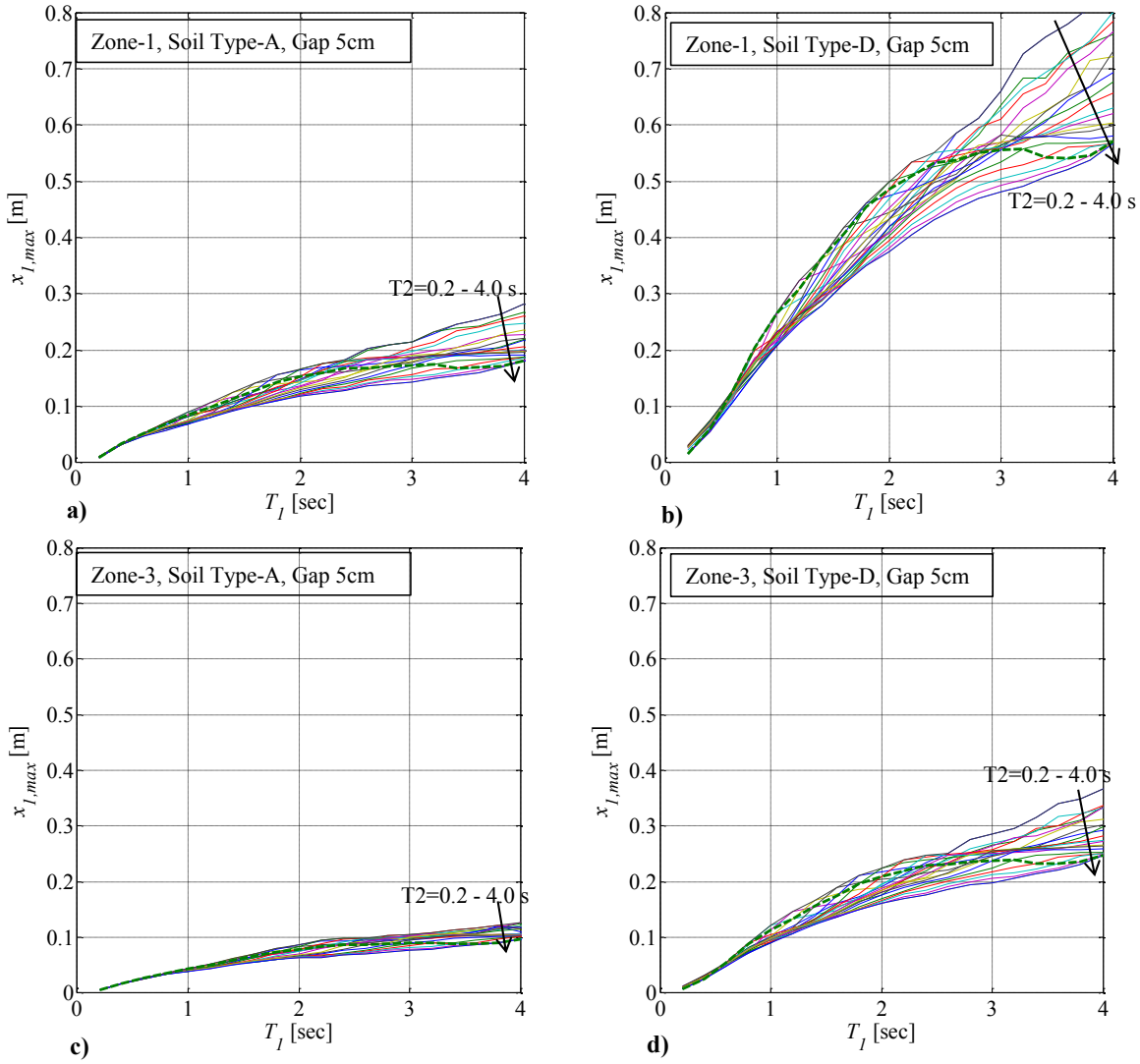

Figure 5: Non-pounding (red dotted line) and pounding displacement response spectra for T2=0.2:0.2:4.0 sec; a) Zone-1, Soil Type-A; b) Zone-1, Soil Type-D; c) Zone-3, Soil Type-A; d) Zone-3, Soil Type-D

In Fig. 6 the pounding force spectrum $F_p(T_1)$, which actually gives also the value of the pounding force affecting the 2nd SDOF in absolute value, is plotted for different values of T_2, for Zone 1 and Soil A. As can be gathered, for values of $T_1 = T_2$, since the two SDOF are actually oscillating on phase, pounding does not occur. Note that, for increasing values of the T the inclination of the increasing branches of the spectrum decreases.

The pounding force spectrum $F_p(T_1)$ is plotted in Fig. 7 for different seismic zones (rows) and soil types (columns) and for increasing values of T_2. The maximum value of the pounding force increases for increasing values of peak ground acceleration, going from zone 1 to zone 3, and for softening mechanical characteristics of the foundation soil (going from class A to D).

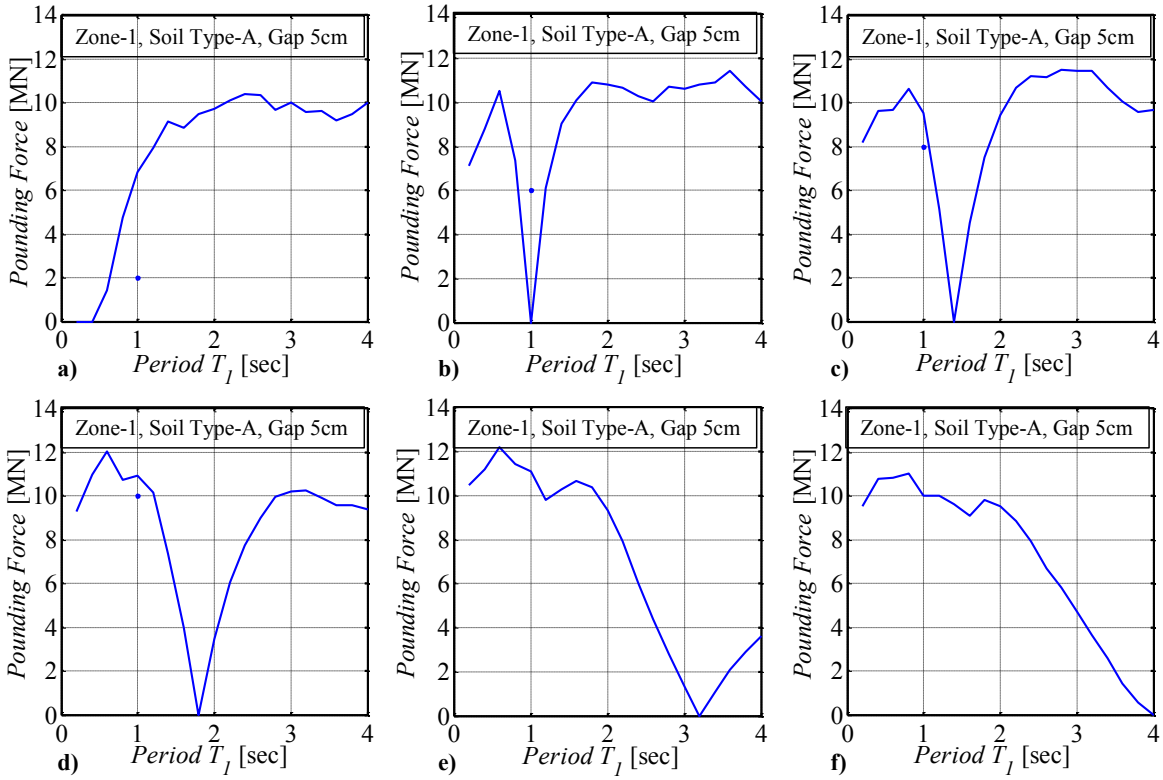

Figure 6: Pounding force response spectrum for Zone-1, Soil Type-A and for different values of T_2: a) $T_2 = 0.2\ sec$; b) $T_2 = 1.0\ sec$; c) $T_2 = 1.8\ sec$; d) $T_2 = 3.2\ sec$; e) $T_2 = 4.0\ sec$.

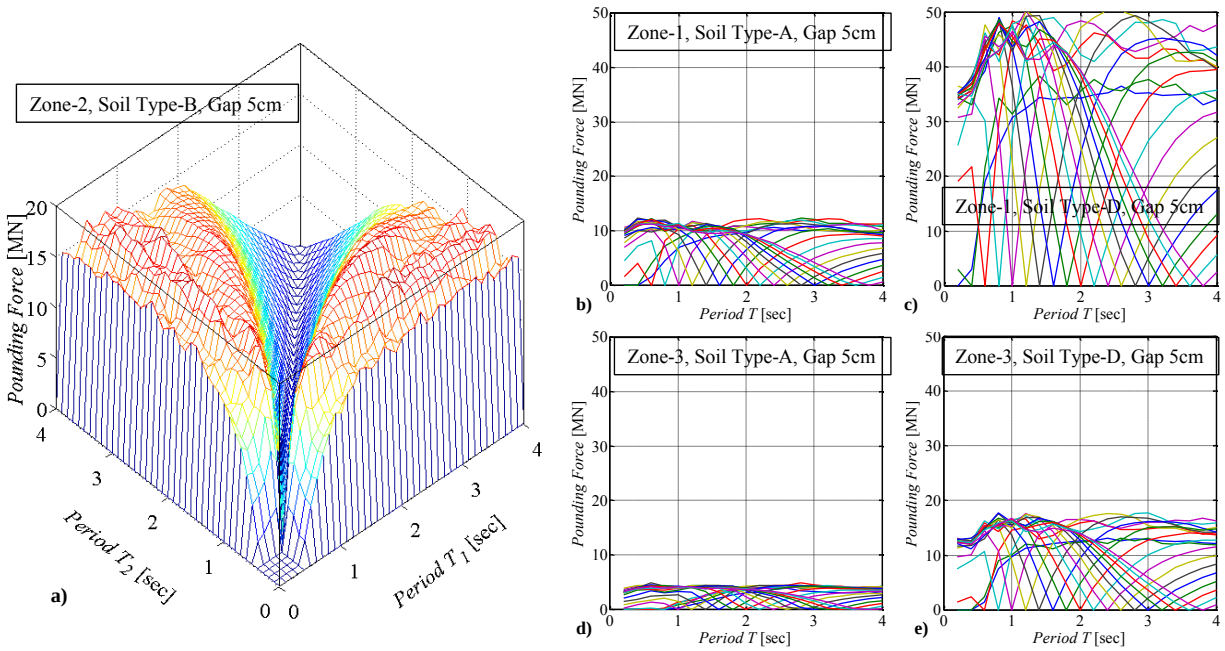

Figure 7: Pounding force response spectra for T2=0.2:0.2:4.0 sec; a) Zone-2, Soil Type-B; b) Zone-1, Soil Type-A; c) Zone-1, Soil Type-D; d) Zone-3, Soil Type-A; e) Zone-3, Soil Type-D.

5 CONCLUSIONS

This paper presented the early results obtained within the work for a Doctoral Thesis concerned with pounding between adjacent bridge structures. In the first part the pounding models available in the literature were analyzed in detail and their differences were highlighted. In the second part of the paper the adopted numerical strategy is described in detail.

In the third and last part of the paper the results obtained by numerical analyses are plotted in terms of both peak displacement spectra and pounding force. It arose that, as expected, spectra are a very effective and slender analytical tool to be used by practitioners concerned with the design of RC bridges in seismic-prone areas. Further developments include the development of equations to correctly predict the above spectra.

REFERENCES

[1] Bertero, V.V., and Collins, R.Cl., (1973), "Investigation of the failures of the Olive View stairtowers during the San Fernando earthquake and their implications on seismic design", Report no. EERC 73-26, Earthquake Engineering Research Center, University of California, Berkeley, CA, 1973.

[2] Earthquake Engineering Research Institute, (1982), "The Central Greece earthquakes of February-March 1981. Reconnaissance and Engineering Report", Report JP-05, Oakland, CA, 1982.

[3] Bertero, V. V., (1987), "Observations on structural pounding", Proc. Int. Conf. Mexico Earthquakes, ASCE, 1987, pp. 264-278.

[4] Hall, J.F., (1995), "Northridge Earthquake of January 17, 1994 - Reconnaissance Report", Vol. 1., Earthquake Spectra; 95-03, Oakland, CA, 1995.

[5] Comartin, C.D., Greene, M., and Tubessing, S.K., (1995), "The Hyogo-Ken Nonbu Earthquake of January 17, 1995- Preliminary Reconnaissance Report", Earthquake Engineering Research Institute, 95-04, Oakland, CA, 1995.

[6] Earthquake Engineering Research Institute. 1999 Chi-Chi, Taiwan, Earthquake Reconnaissance Report, Supplement A to vol. 17. April 2001.

[7] Earthquake Engineering Research Institute. 2001 Bhuj, India Earthquake Reconnaissance Report, Supplement A to vol. 18. July 2002.

[8] C.V.R. Murty, Umesh Dayal, Jaswant N. Arlekar, Sailender K. Chaubey and Sudhir K. Jain; A National Technological Crisis: Structural and Geotechnical damages sustained during M7.9 Bhuj earthquake force. Department of Civil Engineering, IIT Kanpur.

[9] Ruangrassarnee, A., Kawashima, K., (2001), "Relative displacement response spectra with pounding effect", Earthquake Engineering and Structural Dynamics, 2001; 30:1511-38.

[10] C.P. Pantelidis, X. Ma, (1998), "Linear and nonlinear pounding of structural systems", *Computers & Structures*, Vol. 66, No. 1, pp. 79-92, 1998.

[11] Shehata E. Abdel Raheem; Pounding mitigation and unseating prevention at expansion joints of isolated multi-span bridges. *Engineering Structures 31 (2009) 2345-2356.*

[12] S.L. Dimova, Numerical Problems in modeling of collision in sliding systems subjected to seismic excitations. *Advances in Engineering Software*, 31, 2000.

[13] K.T. Chau, X.X. Wei, X. Guo and C.Y. Shen, Experimental and Theoretical simulations of seismic poundings between two adjacent structures. *Earthquake Engineering and Structural Dynamics*, 32(4), 537-554, 2003.

[14] R. Jankowski, Pounding Force response spectrum under earthquake excitation. *Engineering Structures*, 28(8), 1149-1161, 2006.

[15] Kaiming Bi, Hong Hao and Nawawi Chouw. Required separation distance between decks and abutments of a bridge crossing a canyon site to avoid seismic pounding. *Earthquake Engineering and Structural Dynamics*, 39(3), 303-323, 07/2009.

[16] C.J. Athanassiadou, G.G. Penelis, and A.J. Kappos. Seismic response of adjacent buildings with similar or different dynamic characteristics. *Earthquake Spectra*, 10(2), 1994, 293-317.

[17] B. Li, K. Bi, N. Chouw, J.W. Butterworth, and H. Hao. Experimental investigation of spatially varying effect of ground motions on bridge pounding. *Earthquake Engineering and Structural Dynamics*, 2012, 41(14): 1959-1976.

[18] S. Muthukumar, R. DesRoches, (2006), "A Hertz contact model with non-linear damping for pounding simulation", *Earthquake Engineering and Structural Dynamics,* 35(7), 811-828, 2006.

[19] Jankowski, R., (2005), "Non-linear visco-elastic modeling of earthquake-induced structural pounding", *Earthquake Engng Struct. Dyn*., 2005, 34:595–611.

[20] Guo, A., Li, Z., Li H., and Ou, J., (2009) "Experimental and analytical study on pounding reduction of base-isolated highway bridges using MR dampers", Earthquake Engng Struct. Dyn. 2009, 38:1307–1333.

[21] K.T. Chau, and X.X. Wei, "Pounding of structures modelled as non-linear impacts of two oscillators", Earthquake Engineering and Structural Dynamics, 2001; 30:633-651.

[22] Van Mier, J.G., Pruijssers A., Reinhardt, H.W. and Monnier, T., (1991). "Load Time Response of Colliding Concrete Bodies", *Journal of Structural Engineering*, 117(2):354-374.

[23] Mandal, B., "Development of Seismic Response Spectra for bridges including deck hammering", PhD Thesis (in preparation), Department of Structural Engineering and Geotechnics, Sapienza University of Rome, Italy.

[24] Rice, J.R., (1983), Numerical Methods, Software, and Analysis (New York: McGraw-Hill), § 9.2.

[25] Shampine, L.F., Watts, H.A., (1977), "The art of writing a Ringe-Kutta Code, part I", Math. Software III, (J.R. Rice ed.), New York: Academic Press.

[26] SIMQKE_GR.zip, Programmi Gratuiti per Ingegneria Civile (Civil Engineering Free Software) sviluppati con la collaborazione degli studenti Da Piero e Gelfi.

[27] OPCM3274, (2003) "Ordinance of the President of the Council of Ministers", 20 march 2003.